Nitrogen-14 Nuclear Quadrupole Resonance Spectra of the Coordinated Amino Group and of Coordinated Imidazole. Crystal and Molecular Structures of Chloroglycylglycinato(imidazole)cadmium[1]

Carol I. H. Ashby,[2] William F. Paton, and Theodore L. Brown*

Contribution from the School of Chemical Sciences, University of Illinois, Urbana, Illinois 61801. *Received September 6, 1979*

Abstract: The X-ray structure determination of chloroglycylglycinato(imidazole)cadmium reveals approximately octahedral coordination about the metal center. The structure consists of dimers; the coordinating ligands about the metal are chloro, terminal amino, amide carbonyl, imidazole, and bidentate carboxylato. Pertinent crystallographic data: $C_7H_{11}CdClN_4O_3$, space group $P2_1/c$, $a = 7.338$ (1) Å, $b = 16.136$ (1) Å, $c = 11.554$ (1) Å, $\beta = 124.0°$, $Z = 4$, $R_1 = 0.042$ for 3933 reflections with $I > 2\sigma(I)$. The ^{14}N NQR spectra have been obtained at 77 K for glycine, glutamic acid, and histidine complexes involving Zn and Cd, and for glycylglycine complexes of both Zn and Cd. The ^{14}N NQR transitions for coordinated amino group, peptide amide group, and coordinated imidazole are reported. A model for the electric field gradient (efg) parameters at the coordinated amino nitrogen is presented and employed to interpret the spectra of the complexes in terms of the population of the nitrogen orbital directed toward the metal ion. In complexes that also contain coordinated imidazole, the extent of electron transfer from amino nitrogen to the metal center is greater than for the imino nitrogen of imidazole. The ^{14}N NQR data for the amino-type nitrogen of coordinated imidazole reflect predominantly variations in hydrogen bonding rather than the effects of the Lewis acid center bound to the imino nitrogen. The quadrupole coupling constant of the amide nitrogen in glycylglycine increases upon complex formation, whereas it might have been expected to decrease.

Interactions of metal ions with biologically important compounds such as amino acids and peptides are of great interest because of the widespread occurrence of metal ions in biological systems. Metal ions are of established importance in the functioning of many enzymes; moreover, the interactions of metal ions with nonenzymatic proteins are numerous.[3] For example, transport of zinc and copper in blood involves complexes with serum albumin and amino acids.[4] The interactions of small peptides such as glutathione with metal ions have generated considerable interest.[5] In nonbiological systems, the reactivities of amino acids and peptides are modified by metal ions.[6] Proton exchange, racemization, and aldol condensation at the α carbon occur due to alteration of the electron distribution resulting from coordination of the amino group to a metal ion.

It is therefore of interest to study changes in the electronic environments of nitrogen in metal complexes of amino acids or peptides as compared with the free ligands. Nuclear quadrupole resonance (NQR) spectroscopy provides an excellent probe of electronic environment about ^{14}N. Several previous studies of the NQR spectra of uncoordinated amino acids and peptides have been reported.[7-14] We have studied the ^{14}N NQR spectra of complexes of amino acids and glycylglycine with the diamagnetic metals zinc and cadmium, to examine the effect of coordination upon the electronic environment of the donor nitrogen atoms.

Experimental Section

Materials. Bis(glycinato)zinc monohydrate and bis(glycinato)-cadmium monohydrate, $M(Gly)_2 \cdot H_2O$, were prepared as previously reported.[15]

Anal. Calcd for $Zn(Gly)_2 \cdot H_2O$: C, 20.78; H, 4.33; N, 12.12; Zn, 28.14. Found: C, 20.94; H, 4.25; N, 12.07; Zn, 28.53. Calcd for $Cd(Gly) \cdot H_2O$: C, 17.27; H, 3.60; N, 10.07. Found: C, 17.36; H, 3.59; N, 10.12.

L-Glutamatozinc Dihydrate and L-Glutamatocadmium Dihydrate, M(L-Glu)·2H₂O. Freshly prepared metal hydroxide was added to a hot solution of glutamic acid in a 1:2 molar ratio. Crystals deposited upon cooling. Alternative preparations have been reported.[16]

Anal. Calcd for $Zn(L\text{-}Glu) \cdot 2H_2O$: C, 24.19; H, 4.44; N, 5.64; Zn, 26.21. Found: C, 24.24; H, 4.59; N, 5.87; Zn, 26.22. Calcd for $Cd(L\text{-}Glu) \cdot 2H_2O$: C, 20.48; H, 3.75; N, 4.78; Cd, 38.23. Found: C, 20.65; H, 3.91; N, 4.78; Cd, 38.04.

Bis(L-histidinato)zinc Dihydrate, Zn(L-His)₂·2H₂O. Zinc oxide was added slowly to an aqueous solution of histidine in a 1:2 molar ratio. Undissolved material was removed by filtration. Ethanol was added to the filtrate slowly until the solution became turbid. Needles formed upon standing.

Anal. Calcd for $Zn(L\text{-}His)_2 \cdot 2H_2O$: C, 35.21; H, 4.89; N, 20.54; Zn, 15.89. Found: C, 35.49; H, 4.89; N, 20.79; Zn, 16.10.

Haloglycylglycinato(imidazole)cadmium, Nitratoglycylglycinato(imidazole)cadmium, and Nitratoglycylglycinato(imidazole)zinc, M(Glygly)(Im)X. The mixed complexes of glycylglycine and imidazole with zinc and cadmium were prepared using the appropriate metal salt in a manner analogous to that previously reported for the chloride.[17] The cadmium nitrate complex was not hydrated, as previously reported; both nitrato complexes crystallized only after long standing.

Anal. Calcd for Cd(Glygly)(Im)Cl: C, 24.24; H, 3.17; N, 16.16; Cd, 32.32. Found: C, 24.26; H, 3.26; N, 15.85; Cd, 32.76. Calcd for Cd(Glygly)(Im)Br: C, 21.48; H, 2.81; N, 14.32; Cd, 28.64. Found: C, 21.12; H, 2.65; N, 14.20; Cd, 28.41. Calcd for Cd(Glygly)(Im)-(NO_3): C, 22.58; H, 2.69; N, 18.82; Cd, 30.11. Found: C, 22.38; H, 2.83; Cd, 30.08. Calcd for Zn(Glygly)(Im)(NO_3): C, 25.74; H, 3.37; N, 21.45; Zn, 20.04. Found: C, 23.45; H, 3.10; N, 21.49; Zn, 18.32.

The NQR spectra were obtained at 77 K using the double-resonance techniques described previously.[18,19]

Results

Crystal Data for Chloroglycylglycinato(imidazole)cadmium. $C_7H_{11}CdClN_4O_3$, mol wt 347.0, monoclinic, $a = 7.338$ (1) Å, $b = 16.136$ (1) Å, $c = 11.554$ (1) Å, $\beta = 124.02$ (1)°, $V = 1133.9$ Å^3, $Z = 4$, $\rho_c = 2.03$ g cm^{-3}, μ(Mo Kα) = 21.5 cm^{-1}, $F(000) = 680$, systematic absences for $h0l$ when $l = 2n + 1$ and for $0k0$ when $k = 2n + 1$ establish the space group as $P2_1/c$. The cell dimensions were obtained by a least-squares fit to the automatically centered setting for 29 reflections ($6° < 2\theta < 50°$) on a Syntex $P2_1$ diffractometer equipped with a graphite monochromator, λ(Cu K$\bar{\alpha}$) = 0.710 69 Å.

Solution and Refinement of the Structure. A crystal with dimensions ca. 0.25 × 0.30 × 0.55 mm was used for data collection. The data collection was performed in the 2θ-θ scan mode. The variable scan option was employed (2.0–30.0° min^{-1}) with the total background time equal to 0.25 of the scan time. Three standard reflections were monitored every 57 reflections; examination of these reflections showed no crystal

0002-7863/80/1502-2990$01.00/0

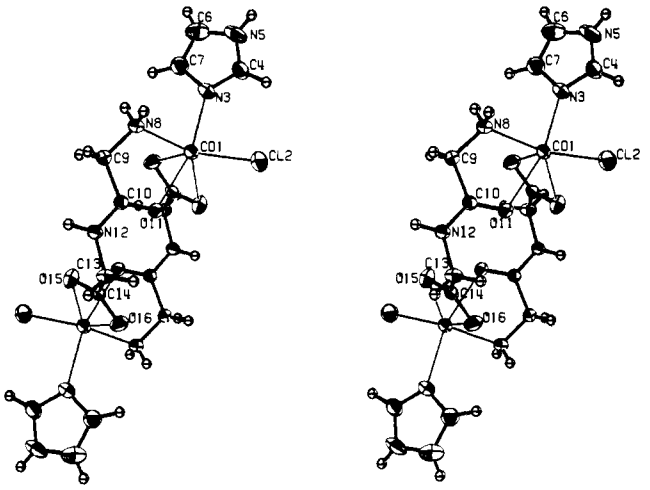

Figure 1. Stereoview of the dimeric unit in Cd(Glygly)(Im)Cl.

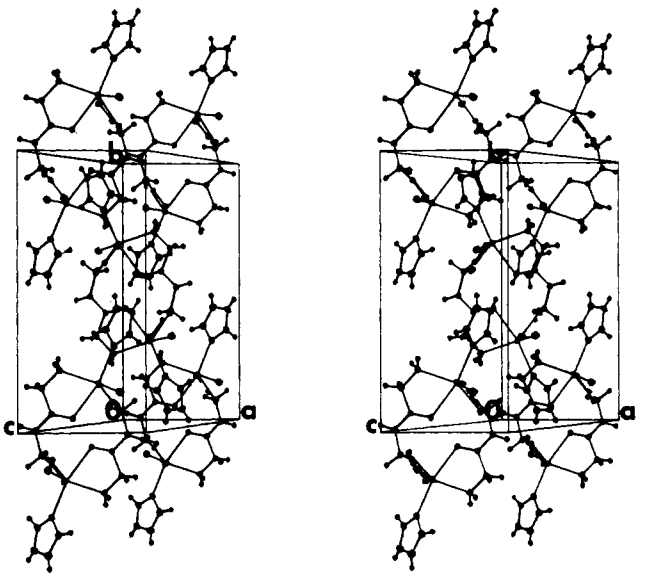

Figure 2. Stereoview of lattice packing in Cd(Glygly)(Im)Cl.

deterioration. The *hkl* and *hkl* octants were collected out to $2\theta = 70°$ ($\sin\theta/\lambda = 0.807$). Out of the possible 5053 unique reflections collected, 3933 were considered significant at the 2σ criterion based on counting statistics. The data were corrected for Lorentz and polarization effects, but not for absorption.

The structure was solved using the Patterson function; a weighted Fourier map based on the trial coordinates for the cadmium atom revealed the positions of the other nonhydrogen atoms. Virtually all crystallographic calculations were carried out on the Syntex EXTL structure determination system. Eight cycles of block-diagonal least-squares refinement, the last five with anisotropic thermal parameters, converged with values for R_1 and R_2 of 0.042 ($R_1 = \Sigma\|F_o| - |F_c\|/\Sigma|F_o|$; $R_2 = [\Sigma(\|F_o| - |F_c\|)^2/\Sigma w|F_o|^2]^{1/2}$). The hydrogen atoms were located from a difference Fourier map and included in the model with isotropic thermal parameters. Continued full-matrix, least-squares refinement of the positional and anisotropic thermal parameters for the nonhydrogen atoms and of the positional and isotropic thermal parameters for the hydrogen atoms converged with values for R_1 and R_2 of 0.037 and 0.030, respectively; the final value of $[\Sigma w(|F_o| - |F_c|)^2/(m-n)]^{1/2}$, where m is the number of observations and n is the number of variables, is 1.93. The scattering curves for the neutral atoms were taken from the analytical expression used in the International Tables for X-ray Crystallography;[20] the curves for cadmium and chlorine were corrected for the effects of anomalous dispersion. The highest electron density in the final difference map is less than 0.8 e Å^{-3}. The final values of the atomic coordinates are given in Table A.[21]

To confirm the orientation of the imidazole ring, the atom types associated with N(5) and C(6) were interchanged and three cycles of full-matrix, least-squares refinement were performed. The thermal parameters for C(6) increased to very large values, indicating that the original choice of the ring orientation is correct.

Description of the Structure. The structure of chloroglycylglycinato(imidazole)cadmium is depicted in Figures 1 and 2. The complex exists in the solid state as a dimer. Each cadmium is coordinated to a chloride ion, the imino nitrogen of an imidazole, the terminal amino nitrogen and peptide oxygen of one glycylglycine, and the two carboxylate oxygens of a second glycylglycine, in a distorted octahedral geometry. The bond lengths and bond angles are listed in Tables I and II. The four hydrogens bound to nitrogen engage in hydrogen bonding with an adjacent dimer; these interactions are listed in Table III. There is no intradimer hydrogen bonding.

NQR Data. The ^{14}N quadrupole resonance transitions for all compounds studied are listed in Tables IV and V. The values listed in parentheses were either not observed or only very weakly observed. These values are calculated from the other two assigned frequencies.

Discussion

The Coordinated Amino Group. To interpret the electric field gradient (efg) parameters of the coordinated amino nitrogen, we have employed a model that utilizes assumptions originally formulated by Townes and Dailey.[22] The efg at nitrogen is assumed to be due solely to electrons in nitrogen valence orbitals that possess p character. The valence orbitals about the nitrogen are assumed to be sp^3 hybrid orbitals. In our model two of these orbitals will be assumed to be employed in equivalent N-H bonds; a third is employed in bonding to carbon, and the fourth orbital is the "donor" orbital. Three approaches to the interpretation of the efg in terms of sp^3 orbital populations at nitrogen have been advanced. Application of two of the methods is severely restricted by the fixed position of the principal axes relative to the molecular framework.[23,24] Therefore, we have employed a modification of the formulation of Edmonds et al.,[7] which accommodates changes in the position of the principal axes relative to the molecular framework. Figure 3 shows how the sp^3 hybrid orbitals are defined in a primed axis system. In this axis system, the following expressions for the components of the electric field gradient tensor may be derived:

$$q_{y'y'} = -\frac{3}{8}(b + c - 2a)q_0$$

$$q_{z'z'} = \frac{3}{8}(b + c - 2a)q_0$$

$$q_{x'x'} = q_{x'y'} = q_{y'z'} = 0 \qquad (1)$$

$$q_{x'z'} = (3/4\sqrt{2})(b - c)q_0$$

The letters a, b, and c represent the nitrogen orbital populations in the N-H, N-C, and N-M bonds, respectively. The quantity q_0 is the field gradient due to a single electron in a nitrogen 2p orbital. We assume $e^2Qq_0/h = 9.0$ MHz, as in previous work.[19,25]

In previous modelings of coordinated nitrogen we have employed as reference compound the free ligand, in which an orbital on nitrogen contains an unshared electron pair.[19,25] Thus the population of the nitrogen donor orbital in the reference compound could be defined as 2. It is not convenient to employ this approach in modeling the coordinated amino

Table I. Bond Lengths (Å) in Cd(Glygly)(Im)Cl

Cd-Cl	2.4708(9)	C(10)-O(11)	1.232(4)
Cd-N(3)	2.303(2)	C(10)-N(12)	1.325(4)
Cd-N(8)	2.309(3)	N(12)-C(13)	1.448(3)
Cd-O(11)	2.421(2)	C(13)-C(14)	1.523(4)
N(3)-C(4)	1.316(5)	C(14)-O(15)	1.252(3)
C(4)-N(5)	1.348(4)	C(14)-O(16)	1.256(3)
N(5)-C(6)	1.353(6)	N(8)-H	0.83(3)
C(6)-C(7)	1.341(5)	N(8)-H′	0.94(3)
C(7)-N(3)	1.381(4)	C(9)-H	0.95(5)
C(4)-H	1.00(4)	C(9)-H′	1.09(4)
N(5)-H	0.82(5)	N(12)-H	0.88(4)
C(6)-H	0.86(3)	C(13)-H	0.99(4)
C(7)-H	0.94(4)	C(13)-H′	0.92(4)
N(8)-C(9)	1.462(4)	Cd-O(15)	2.405(2)
C(9)-C(10)	1.522(4)	Cd-O(16)	2.420(2)

Table II. Bond Angles (deg) in Cd(Glygly)(Im)Cl

Cl-Cd-N(3)	95.47(7)	C(4)-N(3)-C(7)	105.7(3)
Cl-Cd-N(8)	117.99(7)	C(4)-N(3)-Cd	128.4(2)
Cl-Cd-O(11)	97.37(5)	C(7)-N(3)-Cd	125.3(2)
Cl-Cd-O(15)	96.11(5)	N(5)-C(8)-N(3)	110.4(3)
Cl-Cd-O(16)	149.03(6)	$H(C_4)$-C(4)-N(3)	122(2)
N(3)-Cd-N(8)	94.44(9)	C(6)-N(5)-$H(N_5)$	125(3)
N(3)-Cd-O(11)	164.41(8)	C(6)-N(5)-C(4)	107.8(3)
N(3)-Cd-O(15)	110.74(8)	$H(N_5)$-N(5)-C(4)	125(3)
N(3)-Cd-O(16)	84.37(8)	C(7)-C(6)-N(5)	106.6(4)
N(8)-Cd-O(11)	71.71(8)	$H(C_6)$-C(6)-N(5)	126(2)
N(8)-Cd-O(15)	135.53(8)	$H(C_7)$-C(7)-N(3)	121(2)
N(8)-Cd-O(16)	94.83(8)	$H(C_7)$-C(7)-C(6)	129(2)
O(11)-Cd-O(15)	76.63(7)	N(3)-C(7)-C(6)	109.5(3)
O(11)-Cd-O(16)	89.61(7)	C(9)-N(8)-$H(N_8)$	108(2)
O(11)-Cd-O(16)	54.16(7)	C(9)-N(8)-$H'(N_8)$	107(2)
C(9)-N(8)-Cd	114.5(2)	$H(N_8)$-N(8)-$H'(N_8)$	105(3)
$H(N_8)$-N(8)-Cd	108(2)	$H'(N_8)$-N(8)-Cd	114(2)
C(10)-C(9)-$H(C_9)$	108(2)	C(10)-C(9)-$H'(C_9)$	113(3)
$H(C_9)$-C(9)-$H'(C_9)$	101(3)	C(10)-C(9)-N(8)	112.7(2)
$H(C_9)$-C(9)-N(8)	108(2)	$H'(C_9)$-C(9)-N(8)	114(3)
O(11)-C(10)-N(12)	123.2(2)	O(11)-C(10)-C(9)	122.4(2)
Cd-O(11)-C(10)	114.9(2)	N(12)-C(10)-C(9)	114.4(2)
C(13)-N(12)-C(10)	121.1(2)	C(13)-N(12)-$H(N_{12})$	120(2)
C(14)-C(13)-N(12)	114.3(2)	$H(N_{12})$-N(12)-C(10)	119.(2)
O(15)-C(14)-O(16)	122.3(3)	C(14)-C(13)-$H(C_{13})$	104(2)
O(15)-C(14)-C(13)	120.1(2)	C(14)-C(13)-$H'(C_{13})$	107(3)
		O(16)-C(14)-C(13)	117.5(2)

group, because the reference compound is not readily attainable. Rather, we have chosen to employ the zwitterionic form of the amino acid. Thus, in the reference compound M represents the proton; that is, the environment around nitrogen is $C\text{-}NH_3^+$. In the metal complexes the environment around nitrogen is $C\text{-}NH_2M^{2+}$. In all cases the electronic environment about the nitrogen is assumed to possess a plane of symmetry.

The possibility of a nonzero off-diagonal component, $q_{x'z'}$, indicates that the orbital axis system may not be coincident with the principal axis system of the electric field gradient tensor, denoted in Figure 3 by unprimed labels. The principal axis system is related to the orbital axis system by a rotation through the angle θ, about the $y(y')$ axis. This rotation diagonalizes the efg tensor and generates the following relations between the orbital populations and the experimentally determined quadrupole coupling constant, e^2Qq_{zz}/h, and asymmetry parameter, η:[7]

$$(q_{zz}/q_0)(1+\eta) = \frac{3}{4}(b+c-2a)$$

$$(q_{zz}/q_0)(1-\eta/3)\sin 2\theta = (1/\sqrt{2})(b-c) \qquad (2)$$

$$\text{where } \cos 2\theta = (\eta+1)/(3-\eta)$$

When one of the protons in $C\text{-}NH_3^+$ is replaced by a metal ion upon complex formation, a substantial change in c, the nitrogen orbital population in the N-M bond, should result. If we let c_0 be the orbital population of the N-H bond in the zwitterionic form and c the population of the nitrogen orbital in the bond to the metal ion, then we expect that $c - c_0$ should be positive. That is, replacement of a proton by a metal ion will, for most metal ions, result in an increased population of the nitrogen donor orbital. This change should induce concomitant smaller changes in the other nitrogen orbital populations. The new populations are given by the equations

$$a = a_0 - A(c - c_0)$$
$$b = b_0 - B(c - c_0) \qquad (3)$$

where a_0, b_0, and c_0 are the nitrogen orbital populations in the zwitterionic amino acid. We expect that, if the nitrogen donor orbital occupation is increased upon complex formation, as compared with the reference, inductive effects should lead to decreases in the nitrogen populations of the orbitals involving bonding to carbon and the remaining two hydrogens. Thus, the signs of the terms which correct for these inductive effects in eq 3 are negative. The quantities A and B are parametric factors which define the magnitude of the inductive response that causes the a and b populations to change in response to the change in the c population, i.e., a change in the donor orbital occupation.

Substitution of these expressions for a and b into eq 2 yields expressions which relate the quadrupole coupling constant and asymmetry parameter to the change in the nitrogen orbital population of the N-M bond which occurs upon complexation. As in previous studies,[19,25] the model is parametrized in terms of a suitable reference. As indicated above, we have chosen the zwitterionic form of the free amino acid, in which M represents H^+.

We have elected to employ the simplest amino acid, glycine, as reference. The NQR data for three distinct crystallographic forms of glycine, α, β, and γ, have been reported.[10] The three forms differ in the geometry of their hydrogen bonding.[26] The protonated form of the amino group does not exhibit an axially symmetric field gradient because of hydrogen bonding involving one or more of the N-H bonds. However, the hydrogen-bonding pattern of γ-glycine causes the smallest deviation from an assumed *plane* of symmetry; it has therefore been selected as reference. For this $C\text{-}NH_3^+$ group, e^2Qq/h and η are 1.244 MHz and 0.357, respectively.

There exists a range of values for A and B which may be used in eq 3. However, it is desirable to select a single pair of values which are physically and chemically reasonable. In previous studies of pyridine[19] and imidazole[25] complexes, the optimal values for B were found to be 0.08 and 0.11, respectively. The value of B for the amino group should be related to the relative polarizabilities of the N-C σ bonds. In the amino

Table III. Hydrogen-Bonding Interactions in Cd(Glygly)(Im)Cl

bonds	distances, Å	N-H···A angle, deg	acceptor at
N(5)-H···O(11)	N-H 0.82(6) N-O 3.032(4) H-O 2.26(5)	156.5	$(2-x, \frac{1}{2}+y, \frac{1}{2}-z)$
N(8)-H′(N_8)···Cl(2)	N-H 0.83(4) N-Cl 3.289(3) H-Cl 2.50(5)	158.9	$(-1+x, \frac{1}{2}-y, -\frac{1}{2}+z)$
N(8)-H″(N_8)···O(16)	N-H 0.94(4) N-O 3.154(3) N-O 2.14(4)	166.1	$(1-x, \frac{1}{2}+y, \frac{1}{2}-z)$
N(12)-H···O(15)	N-H 0.88(4) N-O 2.861(3) H-O 1.99(4)	169.3	$(\bar{x}, \bar{y}, \bar{z})$

Table IV. ^{14}N Nuclear Quadrupole Resonance Data of Metal-Amino Acid and Metal-Peptide Complexes at 77 K[a]

compd	terminal amino nitrogen					peptide nitrogen				
	ν_+	ν_-	ν_0	e^2Qq/h	η	ν_+	ν_-	ν_0	e^2Qq/h	η
1. $Zn(Gly)_2 \cdot H_2O$	2440	1655	785	2730	0.575					
2. $Cd(Gly)_2 \cdot H_2O$	2607	1729	878	2891	0.607					
3. $Zn(L\text{-}His)_2 \cdot 2H_2O$	2435	1658	777	2729	0.570					
	2373	1596	777	2646	0.587					
4. Cd(Glygly)(Im)Cl	2708	(1833)	875	3040	0.579	2798	2035	763	3222	0.474
5. Cd(Glygly)(Im)Br	2715	(1840)	875	3037	0.576	2787	(2014)	773	3200	0.483
6. $Cd(Glygly)(Im)(NO_3)$	2810	(1895)	915	3136	0.583	2860	(2102)	758	3308	0.468
7. $Zn(Glygly)(Im)(NO_3)$	2570	(1680)	890	2833	0.628	2770	2049	721	3212	0.449
8. $Zn(L\text{-}Glu) \cdot 2H_2O$	2645	1923	722	3045	0.474					
9. $Cd(L\text{-}Glu) \cdot 2H_2O$	2671	1948	723	3075	0.470					
10. Cd(Glygly)(Im)I	2715	(1805)	910	3013	0.640	2812	(2025)	787	3225	0.488

[a] All transition frequencies and e^2Qq/h in kHz.

Table V. ^{14}N NQR Data for Coordinated Imidazole at 77 K

compd	imino nitrogen, N(3)					amino nitrogen, N(1)				
	ν_+	ν_-	ν_0	e^2Qq/h	η	ν_+	ν_-	ν_0	e^2Qq/h	η
$Zn(L\text{-}His)_2 \cdot 2H_2O$	1987	1323	664	2206	0.601	1343	679	664	1348	0.985
Cd(Glygly)(Im)Cl	2107	(1709)	398	2544	0.313	1438	(1040)	398	1652	0.482
Cd(Glygly)(Im)Br	2104	(1714)	390	2545	0.306	1463	(1073)	390	1690	0.461
Cd(Glygly)(Im)I	1947	(1386)	561	2222	0.505	1379	920	459	1532	0.599
$Cd(Glygly)(Im)(NO_3)$	2059	(1654)	405	2475	0.327	1385	(749)	636	1423	0.894
$Zn(Glygly)(Im)(NO_3)$	2119	1542	577	2440	0.473	1348	682	666	1353	0.984

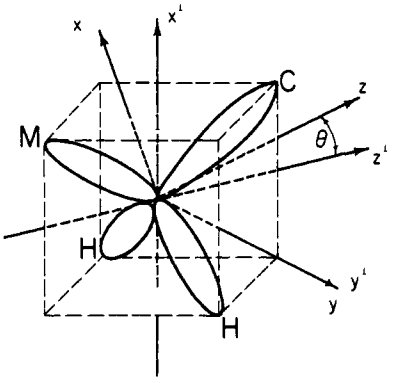

Figure 3. Orbital axis system for the coordinated amino group. The unprimed labels denote the axis system of the efg tensor.

group the nitrogen orbital directed toward C is an approximately sp^3 hybrid rather than sp^2 in the planar aromatic compounds, but this should cause only a small increase in bond polarizability. We thus expect that an appropriate value of B in our amino group model is about 0.11.

It has been estimated that the longitudinal bond polarizability of an N-H bond is 0.58×10^{-24} cm^3 for N-H as compared with 0.86×10^{-24} cm^3 for an N-C σ bond.[27] Thus A should be smaller than B; we assume a value of 0.07 for A, which reflects the inductive response of the N-H bonds. The total inductive response to a unit electron withdrawal from nitrogen in the amino group, $2A + B$, is thus 0.25. This is to be compared with a value of 0.62 for imidazole.[25] The larger value in the latter case is ascribed to the much greater polarizability of the π-electron system, which accounts for 65% of the charge flowing onto nitrogen in response to a unit electron withdrawal.

Having decided upon values for A and B, one can then employ eq 3 and 2 to calculate e^2Qq/h and η as a function of assumed values for $c - c_0$. Inserting the experimental values for γ-glycine, the reference compound for which $c - c_0 = 0$, into eq 2, one obtains expressions for b_0 and a_0 in terms of c_0. When these are inserted into eq 3, a and b are expressed entirely in terms of c_0 and c. At this point we need not specify values for a_0, b_0, and c_0, because we are interested in the *changes* in

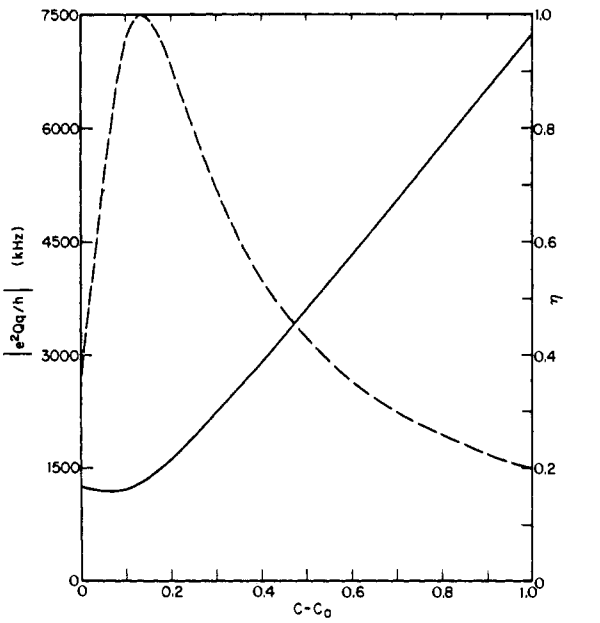

Figure 4. Graph of calculated e^2Qq/h and η vs. the nitrogen-M bond orbital population change, $c - c_0$, for the coordinated amino group. The dotted line represents η, the solid line e^2Qq/h.

populations when a proton in the reference is replaced by another Lewis acid. By substituting the resulting expressions for a and b, based on γ-glycine reference, into eq 2 we obtain a pair of equations in which q_{zz}/q_0 and η are expressed entirely in terms of $c - c_0$. Thus it is possible to generate a graph of e^2Qq_{zz}/h and η vs. a range of assumed values of $c - c_0$.

A plot of the absolute value of the calculated coupling constant vs. the population change $c - c_0$ is superimposed upon the corresponding plot for the calculated asymmetry parameter in Figure 4. As indicated above, the calculated curves are constrained to pass through the experimental values of quadrupole coupling constant and asymmetry parameter of the reference amino acid, γ-glycine, for which $c - c_0 = 0$. That portion of Figure 4 which encompasses the range of experimental data for the metal complexes is shown enlarged in Figure 5.

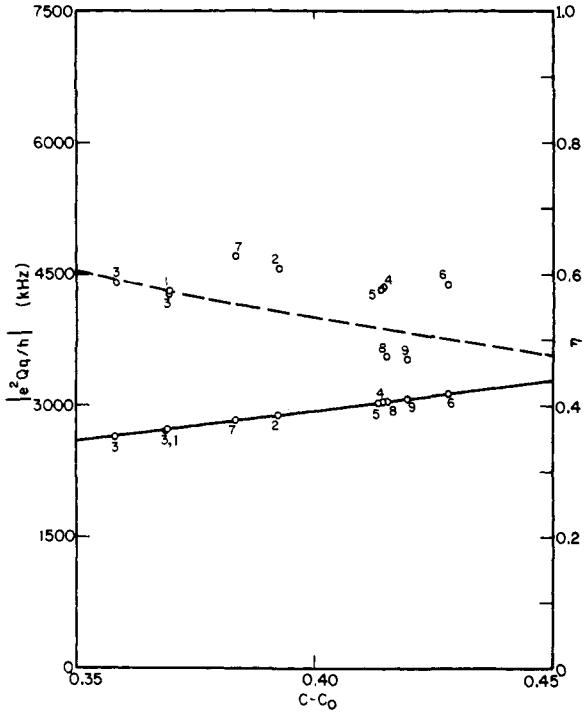

Figure 5. Enlarged portion of Figure 4, with experimental data for coordinated amino groups (Table IV). The dotted line refers to η, the solid line to e^2Qq/h.

Table VI. Changes in Donor Orbital Population for Coordinated Terminal Amino Nitrogen

compd	$c - c_0$
1. $Zn(Gly)_2 \cdot H_2O$	0.371 ± 0.001
2. $Cd(Gly)_2 \cdot H_2O$	0.394 ± 0.027
3. $Zn(L\text{-}His)_2 \cdot 2H_2O$	0.371 ± 0.001
	0.359 ± 0.001
4. Cd(Glygly)(Im)Cl	0.416 ± 0.028
5. Cd(Glygly)(Im)Br	0.415 ± 0.026
6. Cd(Glygly)(Im)(NO_3)	0.430 ± 0.037
7. Zn(Glygly)(Im)(NO_3)	0.386 ± 0.030
8. $Zn(L\text{-}Glu) \cdot 2H_2O$	0.417 ± 0.019
9. $Cd(L\text{-}Glu) \cdot 2H_2O$	0.421 ± 0.011
10. Cd(Glygly)(Im)I	0.412 ± 0.037

In fitting the data for each amino acid and peptide complex to the model one wishes to choose a value for $c - c_0$ that minimizes the deviations of the three efg tensor components q_{xx}, q_{yy}, and q_{zz} calculated from the experimental data from the values of these components based on the model. The lines in Figure 6 show the variations in e^2Qq_{ii}/h ($i = x, y, z$) as a function of $c - c_0$ based on the model, with $A = 0.07$ and $B = 0.11$. The values of e^2Qq_{ii}/h derived from the experimental data using eq 4 are shown as circles. The location of the data set for each nitrogen along the horizontal axis is determined by the minimum in the sum of the squares of vertical deviations from the lines. Invariably, this criterion results in an excellent fit of the major (q_{zz}) component to the lines and in larger, counterbalancing departures in the q_{yy} and q_{xx} components. Thus, the fit of the data for each nitrogen to the e^2Qq/h line in Figure 5 is excellent, whereas the scatter in the fitting of η is much poorer. It is clear from Figure 6 that the optimal value of $c - c_0$ is located with good precision by fitting of the major efg component alone. The values of $c - c_0$ derived from the placements shown in Figure 6 are listed in Table VI.

$$\eta = (q_{xx} - q_{yy})/q_{zz} \qquad (4)$$
$$q_{xx} + q_{yy} + q_{zz} = 0$$

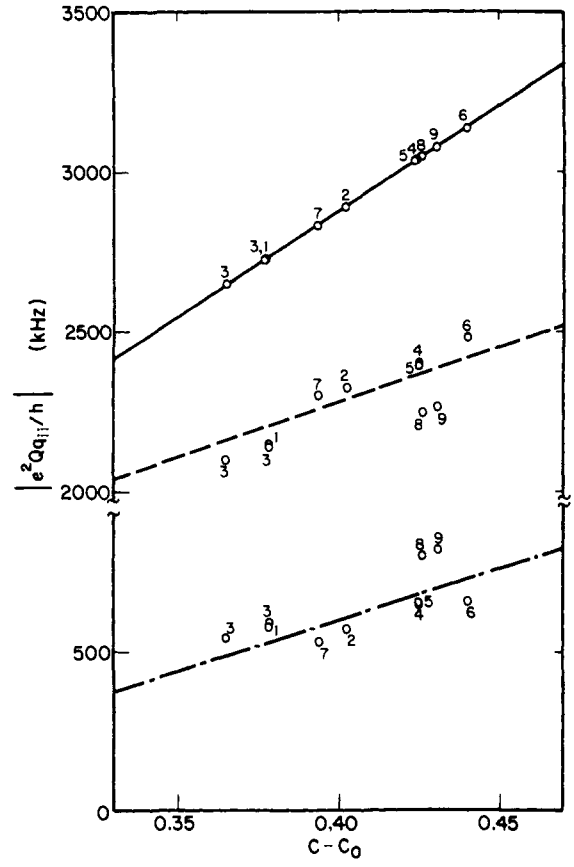

Figure 6. Graph of calculated $|e^2Qq_{ii}/h|$ vs. the nitrogen-M bond orbital population change, $c - c_0$, for coordinated amino groups: e^2Qq_{zz}/h (—); e^2Qq_{yy}/h (– –); e^2Qq_{xx}/h (–·–).

Table VII. Comparison of Donor Orbital Populations at Coordinated and Terminal Amino Nitrogen Atoms in Metal Complexes

compd	donor orbital occupancy, σ	
	amino group	imidazole
Zn(Glygly)(Im)(NO_3)	1.69	1.76
Cd(Glygly)(Im)(NO_3)	1.73	1.80
Cd(Glygly)(Im)Cl	1.72	1.80
Cd(Glygly)(Im)Br	1.72	1.81
Cd(Glygly)(Im)I	1.71	1.74

In fitting the data for the complexes we have assumed that the populations in the amino nitrogen orbitals are not noticeably perturbed by ionization of the carboxylate function, nor by the presence of a peptide amide group. Inequivalence in the N–H bond populations caused by hydrogen bonding is a more likely source of the observed scatter in η. An analogous scatter observed in the data for the amino nitrogen in imidazole complexes can be related to hydrogen-bonding interactions (vide infra). The data for the terminal amino groups of the glutamic acid complexes of zinc and cadmium deviate most markedly from the calculated curves. Examination of the crystal structures[16] reveals that only one of the amino group hydrogens is involved in hydrogen bonding. This would be expected to cause a significant inequivalence in the N–H bonds, in violation of the model assumption. In those complexes of known structure for which the NQR data fit the model, both hydrogens of the NH_2 groups are involved in hydrogen bonding.

From the values of $c - c_0$ for the complexes listed in Table VI it is apparent that there is a correlation between the Lewis acidity of the metal and the change in donor orbital population relative to the reference zwitterion. The more acidic zinc differs

Table VIII. Donor Orbital Populations for the Imino Nitrogen of Coordinated Imidazole

compd	σ	compd[a]	σ
$Zn(L\text{-}His)_2 \cdot 2H_2O$	1.718 ± 0.015	$Cd(Im)_6(NO_3)_2$	1.846 ± 0.001
$Cd(Glygly)(Im)(NO_3)$	1.797 ± 0.015	$[Cd(Im)_2Cl_2]_\infty$	1.758 ± 0.01
			1.756 ± 0.005
Cd(Glygly)(Im)Cl	1.805 ± 0.01	$Zn(Im)_6Cl_2 \cdot 4H_2O$	1.843 ± 0.001
Cd(Glygly)(Im)Br	1.807 ± 0.013	$Zn(Im)_6(NO_3)_2$	1.837 ± 0.003
Cd(Glygly)(Im)I	1.742 ± 0.005	$Zn(Im)_2Cl_2$	1.718 ± 0.001
$Zn(Glygly)(Im)(NO_3)$	1.759 ± 0.018	$Zn(Im)_2(NO_3)_2$	1.684 ± 0.005
			1.684 ± 0.001

[a] All data in this column from ref 25.

less from the reference proton than does cadmium in the isomorphous glycine complexes. The acidity of a single metal ion is modulated by the number and type of ligands bound to it. Comparison of the relative donor abilities of terminal amino nitrogens and imidazole nitrogen may be made by assuming a value for the population, c_0, since $(c - c_0) + c_0 = \sigma$, the donor orbital population in the N–M bond.[25] A reasonable value for c_0 would lie between 1.2 and 1.3 electrons. The corresponding quantity in pyridinium ion is estimated to be 1.43.[28] In imidazole it is estimated to be 1.30.[25] In both these cases the nitrogen employs a nominally sp^2-hybridized orbital as opposed to approximately sp^3 in the amino group. However, since the nitrogen carries a formal 1+ charge, a value of c_0 of about 1.30 seems reasonable. Using this value for c_0, the values for c in Table VII are calculated for the five complexes that contain both coordinated amino and imidazole ligands. In all cases listed, the extent of charge transfer to the metal is a little greater from the amino group than from imidazole; this is consistent with the observation that primary amines are stronger bases than aromatic amines such as imidazole or pyridine.

Coordinated Imidazole. The list of compounds studied, Table IV, includes several that contain coordinated imidazole. Using the model previously advanced for the interpretation of the ^{14}N NQR data for the coordinated imino group of imidazole,[25] the donor orbital populations listed in Table VIII are obtained. Several previously determined values[25] are also listed for comparison purposes.

The σ value for the imino nitrogen of the histidine ligand in $Zn(L\text{-}His)_2 \cdot 2H_2O$ is in the range characteristic of tetrahedrally coordinated zinc complexes rather than octahedrally coordinated species, e.g., the $[Zn(Im)_6]X_2$ complexes. The crystal structure of $Zn(L\text{-}His)_2 \cdot 2H_2O$ reveals coordination of four nitrogen donor atoms in a roughly tetrahedral arrangement, with weaker binding of two carboxylate oxygens through tetrahedral faces.[29,30] An inference about the coordination geometry in the cadmium glycylglycine complexes may also be drawn from the imidazole NQR data. Both $[Cd(Im)_2Cl_2]_\infty$[31] and $[Cd(Im)_6](NO_3)_2$[32] contain six-coordinate cadmium. The σ values assigned to imidazole in the glycylglycine complexes, intermediate between the values assigned for these two species, are indicative of a six-coordinate environment. Cadmium is known to readily achieve coordination numbers of 4, 5, and 6. Therefore, in the complexes of the type Cd(Glygly)(Im)X, the question arises as to whether the anion, X, is coordinated. In Table IX are listed the efg parameters of some analogous pairs of imidazole complexes containing both coordinated and noncoordinated anions. For the species in which the anion is coordinated to the metal, a substantial difference in coupling constant is observed when the anion is changed. On the other hand, little difference is seen when the anion is not coordinated. The difference in efg parameters for the chloro and nitrato cadmium glyclyglycine complexes is sufficient to support the contention that the anion is coordinated. The crystal structure (Figures 1 and 2) verfies this contention in the chloride case.

Table IX. Comparison of NQR Data for the Imino Nitrogen of Coordinated Imidazole in Analogous Pairs of Complexes

compd	e^2Qq/h, kHz	η
Cd(Glygly)(Im)Cl	2544	0.313
$Cd(Glygly)(Im)(NO_3)$	2475	0.327
Coordinated Anion		
$Zn(Im)_2Cl_2$	2126	0.567
$Zn(Im)_2(NO_3)_2$	1963	0.701
	1926	0.689
Noncoordinated Anion		
$Zn(Im)_4(NO_3)_2$	2004	0.681
$Zn(Im)_4(ClO_4)_2$	2019	0.678
	2062	0.602
$Zn(Im)_6Cl_2 \cdot 4H_2O$	2809	0.255
$Zn(Im)_6(NO_3)_2$	2804	0.275

Table X. Deviations of N–M Bond Axis from the In-Plane CNC Angle Bisector in Imidazole Complexes and Uncertainties in Donor Orbital Occupancies, σ

compd	uncertainty in σ	in-plane deviation from CNC bisector, deg	out-of-plane deviation deg
$Zn(Im)_2Cl_2$	0.001	0	1.2
		−1	1.7
$Cd(Im)_2Cl_2$	0.006, 0.013	−1.2	0.9
$Cd(Im)_6(NO_3)_2$	0.001	−3.9	
$Zn(Im)_4(ClO_4)_2$	0.001	−1.3	0.6
	0.005	−1.2	6.0
$Zn(Im)_2(Im^-)(NO_3)$			
Im	0.002	−0.8	3.1
	0.004	0	4.3
Im^-	0.025	+4.6	0.9
	0.025	+2.2	3.3
$Zn(L\text{-}His)_2 \cdot 2H_2O$	0.011	+3.8	0.3
Cd(Glygly)(Im)Cl	0.006	+1.6	6.9
$Zn(Im)_6Cl_2 \cdot 4H_2O$	0.001		3.1[a]

[a] An average of six values ranging from 0.0 to 6.4°.

We have previously observed[25] that a relatively poorer agreement between the observed and predicted efg components may result from angular distortions of the N–M bond from the in-plane bisector of the CNC angle at the imino nitrogen. For those compounds of known structure, the in-plane and out-of-plane deviations of the N–M bond from the in-plane bisector are listed in Table X, along with the estimated uncertainty in the value for σ. (A positive in-plane deviation is taken to mean one that moves the N–M bond axis away from the amino ring nitrogen.) It is noteworthy that the only substantial uncertainties in σ arise in those cases where the in-plane deviation is positive.[34] It is not clear why this particular mode of distortion should lead to a larger discrepancy with the model predictions than any other. However, there is some theoretical basis for the observation, in the results of a molecular orbital

Table XI. Nitrogen N-H Orbital Populations, σ, for the Amino, N(1), Nitrogen of Imidazole

compd	σ	compd	σ
imidazole	1.325 ± 0.007	$Zn(Im)_2(NO_3)_2$	1.288 ± 0.006
L-histidine (monoclinic)	1.318 ± 0.002	$(ImH)(NO_3)$	1.355 ± 0.001
$Cd(Im)_6(NO_3)_2$	1.298 ± 0.006	(ImH)I	1.305 ± 0.008
$Zn(Im)_6Cl_2 \cdot 4H_2O$	1.262 ± 0.001	$Zn(L\text{-}His)_2 \cdot 2H_2O$	1.335 ± 0.001
$Zn(Im)_6(NO_3)_2$	1.291 ± 0.005	Cd(Glygly)(Im)Br	1.256 ± 0.005
$Cd(Im)_2Cl_2$	1.252 ± 0.001	Cd(Glygly)(Im)Cl	1.264 ± 0.005
$Cd(Im)_2Br_2$	1.254 ± 0.005	$Cd(Glygly)(Im)(NO_3)$	1.319 ± 0.001
$Zn(Im)_2(C_6H_4O_2)$	1.378 ± 0.002	Cd(Glygly)(Im)I	1.284 ± 0.012
$Zn(Im)_2Cl_2$	1.273 ± 0.007	$Zn(Glygly)(Im)(NO_3)$	1.335 ± 0.001
$Zn(Im)_2Br_2$	1.237 ± 0.005	$[Zn(Im)_2(Im^-)](NO_3)$	1.315 ± 0.001
$Zn(Im)_2I_2$	1.239 ± 0.006		1.332 ± 0.001
	1.227 ± 0.005		
$Zn(Im)_4(ClO_4)_2$	1.287 ± 0.003		
	1.253 ± 0.004		

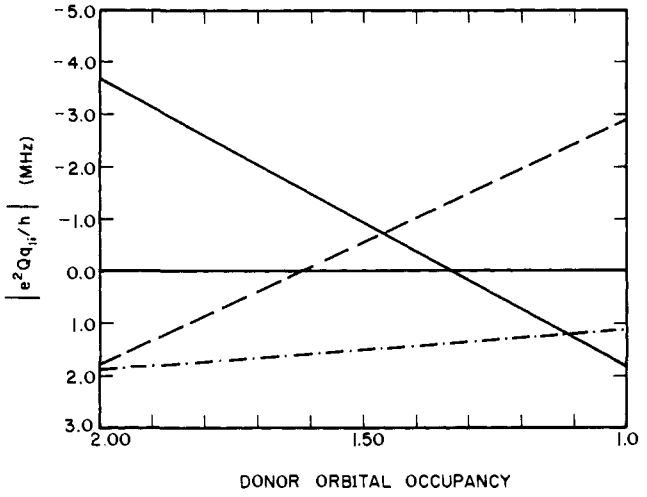

Figure 7. Graph of calculated e^2Qq_{ii}/h vs. donor orbital occupancy for imidazole showing the signs of the efg components: e^2Qq_{zz}/h (—); e^2Qq_{yy}/h (– –); e^2Qq_{xx}/h (–·–).

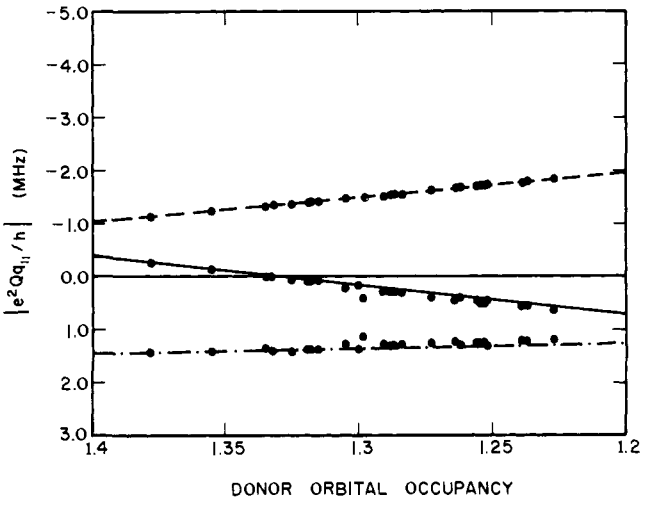

Figure 8. Enlarged portion of Figure 7 with experimental data for amino nitrogen of imidazole.

analysis of the efg parameters in imidazolium ion as a function of the distortions under discussion.[35] In those results a positive in-plane angle deviation of the N-H vector resulted in the largest change in the asymmetry parameter. However, the calculated effects are smaller than those observed for the metal complexes. In any event, the results obtained to date suggest that a relatively poor fit of the imino nitrogen NQR data with the model predictions is most likely to be due to an in-plane distortion of the N-M bond axis away from the amino nitrogen.

The Amino Group of Coordinated Imidazole. In our previous report of the ^{14}N NQR data for coordinated imidazole, no attempt was made to assign a population to the N-H bond of the amino, N(1), nitrogen of the coordinated imidazole. Although the coordinated nitrogen model should apply as well to this case, in which the Lewis acid is H^+, the deviations from the calculated relationships between e^2Qq/h and η as a function of σ seemed large and scattered. It has since become apparent that the best procedure is to seek a least-squares fit between the calculated and observed values for all three efg components.[28] Accordingly we have reexamined the ^{14}N NQR data for the amino group of coordinated imidazole.

A graph of the three calculated efg components for the imidazole-type nitrogen as a function of σ is shown in Figure 7. Figure 8 is an enlargement of that portion of Figure 7 that is appropriate for the experimental data for imidazole N(1); it shows all the imidazole N(1) data from the previous study[25] as well as the new results reported here. It is evident that the data can in fact be fitted very well to the calculated lines; the resulting values of σ are listed in Table XI. (Recall that in this case σ represents the nitrogen orbital population in the N-H bond.) Note that the uncertainties in choice of σ values are quite small. The typical uncertainty in σ is about 0.005, as compared with the total range of 0.15 among all the compounds. It would thus appear that the variations in σ values can be attributed to variations in the electronic environment of the N(1) nitrogen.

According to the model, for σ values less than 1.33, the major (Z) axis of the field gradient tensor lies normal to the plane of the imidazole ring. However, for the compounds for which σ is greater than 1.33 the Z axis of the efg tensor lies along or near the N-H bond. The principal factor in determining σ for the N(1) nitrogen is the strength of its hydrogen bonding to adjacent centers. Larger values of σ correspond to an increase in the electron population in the N(1) orbital due to stronger hydrogen-bonding interaction. This is the kind of effect one expects from a molecular orbital model of the hydrogen bond.[36,37] Correlations with IR spectral and structural data provide a good support for the notion that hydrogen bonding is the environmental variable of major importance.[25,28] One might also look for an effect at the N(1) nitrogen of Lewis acid binding at the imino, or N(3), nitrogen. The best that can be said, however, is that the effects of variation in the Lewis acid bound to N(3) which must be relayed to N(1) through the bond system of the ring seem to be smaller than variations in hydrogen bonding.

The Amide Nitrogen of Coordinated Peptides. The study of the Zn and Cd complexes of glycylglycine provides the first opportunity to observe the effects of coordination on the efg

parameters of the amide nitrogen. In general, this nitrogen is not coordinated, and one might expect that only minor changes in electronic environment should occur. Table XII lists the ^{14}N NQR data and efg parameters for the glycyl amide function in free peptides and in the metal complexes of glycylglycine. There is a substantial and regular increase in e^2Qq/h in the complexes as compared with the free ligand.

The oxygen, nitrogen, and carbon atoms of the peptide group are normally coplanar, and the lone pair on nitrogen forms part of a π-electron system with the carbonyl group. The substantial double-bond character in the N-C(carbonyl) bond of glycylglycine is evidenced by a shortening of this bond by approximately 0.1 Å compared to a single N-C bond length.[39,40] The p_π orbital of the amide nitrogen should have the largest population of the nitrogen valence orbitals. One thus expects that the Z axis of the efg tensor at this nitrogen will lie normal to the plane of the peptide group.

The electron distribution in the π-electron system of the amide group can be roughly described in terms of structures **1** and **2.** Coordination of the carbonyl oxygen to a metal ion

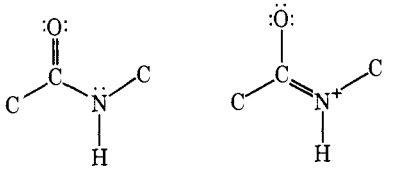

1 2

center, as occurs in the complexes of gylcylglycine (e.g., see Figures 1 and 2), should result in an increased importance for structure **2.** This in turn would suggest that the quadrupole coupling constant at the amide nitrogen should decrease because of a smaller population of the p_π orbital. Instead, we observe an increase of about 10% upon complex formation, in several different but related complexes.

The unexpected increase in e^2Qq/h for the amide nitrogen complex formation is probably related to differences in hydrogen-bonding interactions in the free ligand as compared with the complexes. The crystal-structure evidence for α-glycylglycine shows that the amide proton forms a hydrogen bond to a peptide oxygen. In the structure of Cd(Glygly)(Im)Cl, hydrogen bonding occurs to a metal-bound carboxylate oxygen. The N···O distance is shorter in Cd(Glygly)(Im)Cl (2.861 Å) than in α-glycylglycine (2.959 Å),[39,40] and the N-H···O group more linear (169 vs. 159°). These structural evidences point to a stronger hydrogen-bonding interaction in the metal complexes than in the free ligand. But a stronger hydrogen-bonding interaction should increase the nitrogen N-H bond orbital population, with the result that e^2Qq/h at the amide nitrogen should be still lower. Thus, no obvious explanation for the observed trend is at hand. (The observed changes can be accounted for if we postulate that the coordinated carboxylate oxygen in the complex, because of its interaction with the metal center, is a substantially poorer base toward the N-H proton than the peptide oxygen, the smaller N···O distance notwithstanding.) It will probably be necessary to determine the orientation of the efg axes at the amide nitrogen via a single-crystal study before the problem can be solved.

In summary, this study of the ^{14}N NQR spectra of amino acid and glycylglycine complexes of Zn and Cd provides the first observations of electric field gradient data for the coordinated amino group and for the peptide amide group adjacent to coordinated carbonyl. In addition, substantial new results relating to coordinated imidazole, with regard to both the coordinated imino nitrogen and the amino-type nitrogen of this ligand, have been presented. From these studies it is evident that the efg parameters at coordinated nitrogen atoms are a sensitive indicator of binding to the metal centers, and that rather detailed inferences regarding the extent of electron transfer can be made from the NQR data. Aside from their inherent interest, these results will provide a valuable reference base for the interpretation of ENDOR spectra that reveal the efg parameters for the coordinated nitrogen atoms.

Table XII. The ^{14}NQR Spectra of Amide Nitrogen

compd	ν_+	ν_-	ν_0	e^2Qq/h	η
Glygly[a]	2505	1975	620	3030	0.41
Glyglygly[a]	2620		720	3010	0.48
	2900		1175	3080	0.76
poly-gly[b]	2910		1175	3097	0.76
Cd(Glygly)(Im)NO_3	2860	(2102)	758	3308	0.468
Cd(Glygly)(Im)Cl	2798	2035	763	3222	0.474
Cd(Glygly)(Im)Br	2787	(2014)	773	3200	0.483
Cd(Glygly)(Im)I	2812	(2025)	787	3225	0.488
Zn(Glygly)(Im)NO_3	2770	2049	721	3212	0.488

[a] Reference 13. [b] Reference 12b. [c] Reference 12

Supplementary Material Available: Crystallographic data for chloroglycylglycinato(imidazole)cadmium, atomic coordinates, thermal ellipsoid parameters and structure factor amplitudes, and data relating to selected best planes (35 pages). Ordering information is given on any current masthead page.

References and Notes

(1) This research was supported by Research Grant GM-23395 from the Institute of General Medical Sciences, National Institutes of Health.
(2) National Science Foundation Fellow, 1975-1978; University of Illinois Fellow, 1978-1979.
(3) (a) Boyer, P. D. "The Enzymes", 3rd ed.; Academic Press: New York, 1970. (b) Sigel, H. "Metal Ions in Biological Systems"; Marcel Dekker: New York, 1973.
(4) (a) Giroux, E. L.; Henkin, R. I. *Biochim. Biophys. Acta* **1972**, *273*, 64. (b) Hallman, P. S.; Perrin, D. D. *Biochem. J.* **1971**, *121*, 549.
(5) (a) Kosower, N. S.; Kosower, E. M. In "Free Radicals in Biology", Pryor, W. A., Ed.; Academic Press: New York, 1976; Vol. 2, p 55. (b) Fuhr, B. J.; Rabenstein, D. L. *J. Am. Chem. Soc.* **1973**, *95*, 6944.
(6) (a) Pasini, A.; Casella, L. *J. Inorg. Nucl. Chem.* **1974**, *36*, 2133. (b) Phipps, D. A. *J. Mol. Catal.* **1979**, *5*, 81.
(7) Edmonds, D. T.; Hunt, M. J.; Mackay, A. L. *J. Magn. Reson.* **1973**, *9*, 66.
(8) Hunt, M. J.; Mackay, A. L. *J. Magn. Reson.* **1974**, *15*, 402.
(9) Edmonds, D. T.; Summers, C. P. *J. Magn. Reson.* **1973**, *12*, 134.
(10) Edmonds, D. T.; Summers, C. P. *Chem. Phys. Lett.* **1976**, *41*, 482.
(11) Blinc, R.; Mali, M.; Osredkar, R.; Prelesnick, A.; Zupanic, I.; Ehrenberg, L. *Chem. Phys. Lett.* **1971**, *9*, 85.
(12) (a) Blinc, R.; Mali, M.; Osredkar, R.; Prelesnik, A.; Seliger, J.; Zupancic, I.; Ehrenberg, L. *J. Chem. Phys.* **1972**, *57*, 5087. (b) Blinc, R.; Mali, M.; Osredkar, R.; Seliger, J.; Ehrenberg, L. *Chem. Phys. Lett.* **1974**, *28*, 158.
(13) Edmonds, D. T.; Speight, P. A. *Phys. Lett. A* **1971**, *34*, 325.
(14) Andersson, L.-O.; Gourdji, M.; Guibé, L.; Proctor, W. G. *C. R. Acad. Sci., Ser. B* **1968**, *267*, 803.
(15) Low, B. W.; Hirshfeld, F. L.; Richards, F. M. *J. Am. Chem. Soc.* **1959**, *81*, 4412.
(16) (a) Gramaccioli, C. M. *Acta Crystallogr.* **1966**, *21*, 600. (b) Soylu, H.; Ülkii, D.; Morrow, J. C. *Z. Kristallogr., Kristallgeom., Kristallphys., Kristallchem.* **1974**, *140*, 281.
(17) Rao, G. N.; Li, N. C. *Can. J. Chem.* **1966**, *44*, 1637.
(18) Edmonds, D. T. *Phys. Rep.* **1977**, *29*, 233.
(19) Hsieh, Y.-N.; Rubenacker, G. V.; Cheng, C. P.; Brown, T. L. *J. Am. Chem. Soc.* **1977**, *99*, 1384.
(20) Ibers, J. A., Hamilton, W. C., Eds. "International Tables for X-ray Crystallography", Vol. IV; Kynoch Press: Birmingham, England, 1974; pp 71-147.
(21) See paragraph at end of paper regarding supplementary material.
(22) Townes, C. H.; Dailey, B. P. *J. Chem. Phys.* **1949**, *17*, 782.
(23) Onda, S.; Harada, H.; Nakamura, D.; Kubo, M. *J. Magn. Reson.* **1972**, *8*, 238.
(24) Marino, R. A.; Oja, T. *J. Chem. Phys.* **1972**, *56*, 5453.
(25) Ashby, C. I. H.; Cheng, C. P.; Brown, T. L. *J. Am. Chem. Soc.* **1978**, *100*, 6057.
(26) Iitaka, Y. *Acta Crystallogr.* **1961**, *14*, 1.
(27) Smith, J. W. "Electric Dipole Moments"; Butterworth: London, 1955.
(28) Rubenacker, G. V.; Brown, T. L. *Inorg. Chem.* **1980**, *19*, 392.
(29) Kretsinger, R. H.; Cotton, F. A.; Bryan, R. F. *Acta Crystallogr.* **1963**, *16*, 651.
(30) Kistenmacher, T. J. *Acta Crystallogr., Sect. B* **1972**, *28*, 1302.
(31) Flook, R. J.; Freeman, H. C.; Hug, F.; Rosalky, J. M. *Acta Crystallogr., Sect. B* **73**, *29*, 903.
(32) Mighell, A. D.; Santoro, A. *Acta Crystallogr., Sect. B* **1971**, *27*, 2089.
(33) Ashby, C. I. H.; Cheng, C. P.; Duesler, E. N.; Brown, T. L. *J. Am. Chem. Soc.* **1978**, *100*, 6063.
(34) The sole exception is one of the sites in $Cd(Im)_2Cl_2$. According to the room temperature crystal structure[31] there is but one crystallographically distinct

imidazole, and the angular deviation for this one is negative. We observe two distinct sets of ^{14}N imino nitrogen signals at 77 K. There is possibly a phase transition between room temperature and 77 K.
(34) Dreyfus, M.; Pullman, A. *Theor. Chim. Acta* **1970**, *19*, 20.
(35) McCullen, W. L.; Brown, T. L. *J. Phys. Chem.* **1977**, *81*, 2676.
(36) Kollman, P. A.; Allen, L. C. *Chem. Rev.* **1972**, *72*, 283.
(37) Allen, L. C. *J. Am. Chem. Soc.* **1977**, *99*, 8118.
(38) Ashby, C. I. H. Ph.D. Thesis, University of Illinois, Urbana, Ill., 1979.
(39) Biswas, A. B.; Hughes, E. H.; Shaima, B. D.; Wilson, J. N. *Acta Crystallogr., Sect. B* **1968**, *24*, 40.
(40) Freeman, H. C.; Paul, G. L.; Sabine, T. M. *Acta Crystallogr., Sect. B* **1970**, *26*, 925.

Ternary Complexes in Solution. 35.[1] Intramolecular Hydrophobic Ligand–Ligand Interactions in Mixed Ligand Complexes Containing an Aliphatic Amino Acid

Beda E. Fischer and Helmut Sigel*

Contribution from the Institute of Inorganic Chemistry, University of Basel, CH-4056 Basel, Switzerland. *Received October 10, 1979*

Abstract: Mixed ligand complexes of the type $M(Ar)(Aa)^+$, where $M^{2+} = Cu^{2+}$ or Zn^{2+}, Ar = 2,2′-bipyridyl (bpy) or 1,10-phenanthroline (phen), and Aa^- = alaninate, 2-aminopropionate (α-aminobutyrate), norvalinate, norleucinate, valinate, leucinate (leu), or isoleucinate, have been studied by potentiometric pH titrations and ^1H NMR. The potentiometric measurements reveal a slightly higher formation tendency, expressed as $\Delta \log K_M = \log K^{M(Ar)}_{M(Ar)(Aa)} - \log K^{M}_{M(Aa)}$, for the systems with leucinate as amino acid compared to those with alaninate. This increase in stability is attributed to an intramolecular hydrophobic ligand–ligand interaction between the aromatic ring system of bpy or phen and the isopropyl group of leucine. The position of the intramolecular isomeric equilibrium between an "open" and "closed" form, in which the hydrophobic interaction occurs, was estimated; e.g., the ternary $Zn(phen)(leu)^+$ complex exists about 26% in the folded, i.e., closed, form. ^1H NMR shift measurements of the mentioned systems in the absence and presence of Zn^{2+} confirmed that such hydrophobic ligand–ligand interactions exist and that they are promoted by the formation of a metal-ion bridge between the two reactants. The longer the side chain of the aliphatic amino acid, the larger is the upfield shift of the terminal methyl group(s), resulting from the interaction with the aromatic moiety within the ternary complex. These results prompted a literature search and it became evident that, e.g., M(phenylalaninate)(tyrosinate) or M(phenylalaninate)(norvalinate) have an enhanced stability, compared with M(phe)(ala) or M(phe)(gly), and this is now attributed to intramolecular aromatic-ring stacking and hydrophobic ligand–ligand interactions. For these and other systems (in total about 40) the percentages of the "closed" isomer were calculated; they cover the whole range till up to about 90%. The $\Delta G°$ values calculated from the equilibrium constants agree well with the theoretical predictions for such interactions. Possible biological implications are shortly discussed.

Hydrophobic interactions are known to occur among other noncovalent interactions in biomolecules;[2] they contribute, e.g., in proteins through the interaction of the side chains of the amino acid residues to the formation of distinct structural features.[3] Such hydrophobic interactions occur between two aliphatic groups, or between aliphatic and aromatic moieties; the ring stacking between two aromatic systems is also often listed within this category. With regard to metal ion complexes of low molecular weight, Pettit and Hefford[4] have recently described the situation rather precisely: "Hydrophobic interactions cannot be classified as bonds but they are important, not well understood, and often misused. Although the existence of the interactions is not in doubt,[5] their relevance to the complexes of organic molecules in aqueous solution is not clear". To help to clarify this unsatisfactory situation the present study on ternary complexes was undertaken.

Aromatic ring stacking has been observed in ternary complexes[6,7] formed by two different ligands which contain aromatic rings.[1b,8-11] At least one of these rings has to be incorporated in a flexible side chain, as in trytophanate[1b,8,12] or adenosine 5′-triphosphate,[8-10,12] that a stack may be formed; the other ring may also be of the flexible type, or it may be rigidly fixed to the metal ion as it is the case with 2,2′-bipyridyl or 1,10-phenanthroline.[9,10] Such aromatic ring stacking interactions may enhance the stability[8,10,11] of the ternary complex, but more important they create specific structures,[6,12] because the whole species may also be viewed as a metal ion bridged stacking adduct. In addition these species may be considered as relatively simple models for ternary enzyme/metal ion/ATP[13,14] or enzyme/metal ion/inhibitor[15] complexes.

Hydrophobic ligand–ligand interactions between the aliphatic side chains in ternary complexes containing functionalized cyclodextrins[16] have been studied with the aim to enhance the reactivity of the system. There is so far, to our knowledge, only a single study[17] which considers the stability and the structure of such mixed ligand complexes simultaneously: it was shown that an association of the aliphatic chains of carboxylate and sulfonate ligands with the aromatic rings of bpy or phen[14] within ternary metal ion complexes may occur. But it should also be noted in this connection that for binary (metal-free) systems a hydrophobic interaction between the aromatic moiety of phenols and the aliphatic residue of carboxylic acids has been described.[18] Moreover, it has been suggested "that hydrophobic bonds may be responsible for the increasing stabilization with chain length of the carboxylic acid dimers".[19]

The mentioned results stimulated us to examine the influence of the hydrophobic interaction between an aliphatic and an aromatic group on the stability of ternary Cu^{2+} and Zn^{2+} complexes more in detail, with the aim to quantify the extent of this interaction at least partly. As the hydrophobic interaction is important in nature, amino acids with aliphatic side chains were chosen; as aromatic ligands bpy and phen were taken, because these ligands[20] and their binary complexes[21] are well characterized, and most important the structure of this half of the mixed ligand complex which contains these aromatic ligands is unequivocally defined owing to the rigidity of bpy and phen when coordinated. The amino acids were selected

0002-7863/80/1502-2998$01.00/0